

*Electronic Supplementary Information*

# A Novel Strategy to Simultaneously Tailor Morphology and Electronic Structure of CuCo Hybrid Oxides for Enhanced Electrocatalytic Performance in Overall Water Splitting

Lingjie Li, ‡<sup>a</sup> Liu Cao, ‡<sup>a</sup> Qiudong He,<sup>a</sup> Bo Shang,<sup>a</sup> Jinlong Chen,<sup>a</sup> Jinglei Lei,<sup>\*a</sup>

Nianbing Li,<sup>b</sup> Fusheng Pan<sup>c</sup>

<sup>a</sup> School of Chemistry and Chemical Engineering, Chongqing University, Chongqing, 400044 PR China;

<sup>b</sup> School of Chemistry and Chemical Engineering, Southwest University, Chongqing, 400715 PR China;

<sup>c</sup> School of Materials Science and Engineering, Chongqing University, Chongqing, 400044 PR China.

‡ These authors contributed equally to this work.

\* Corresponding author. Jinglei Lei. Tel.: +86 13983064116; Fax: +86 23 65112328; E-mail address:

JLLei@cqu.edu.cn.

## Table of Contents

### S1. More experimental details:

1.1 Evaluation on electrocatalytic performance ----- 3

1.2 Main reactions during the synthesis process of CeO<sub>2</sub>-CuCoO ----- 4

### S2. More calculation details

2.1 Oxygen evolution reaction on the surface----- 5-6

2.2 Hydrogen evolution reaction on the surface----- 7

S3. Additional figures and tables----- 8-18

References----- 19-21

## **S1. More experimental details:**

### *1.1 Evaluation on electrocatalytic performance*

In order to obtain an accurate potential, the Hg/HgO reference electrode was calibrated in H<sub>2</sub>-saturated 1 M KOH by cyclic voltammetry method. In this experiment, two Pt wires was used to working and counter electrodes, and the Hg/HgO electrode served as the reference electrode. Measuring hydrogen oxidation/evolution at a platinum wire electrode and defining the point of zero current as 0 V versus reversible hydrogen electrode (RHE). In this experiment, the potentials were calculated with respect to RHE by the equation:  $E_{\text{RHE}} = E_{\text{Hg/HgO}} + 0.933 \text{ V}$ .

We got OER and HER Tafel slopes trough the corresponding LSV date, and the values were calculated by the equation:  $\eta = a + b \cdot \log J$ , where  $\eta$  is the overpotential,  $a$  is the overpotential at the current density of 1 mA cm<sup>-2</sup>,  $b$  is the Tafel slope and  $J$  is the current density. Electrochemical impedance spectra (EIS) were carried out at 1.55 V (vs. RHE) for OER and -0.2 V (vs. RHE) for HER, with a frequency range from 100 kHz to 0.01 Hz and 5 mV ac dither. The electrochemical active surface areas (ECSA) were calculated according to the equation:  $\text{ECSA} = C_{\text{dl}}/C_s \times \text{ASA}$ , where  $C_{\text{dl}}$  is the double layer capacitance,  $C_s$  is the specific capacitance of the sample and ASA is the actual surface area of the electrode. In this work, the value of  $C_s$  is estimated to be 0.04 mF cm<sup>-2</sup>. The  $C_{\text{dl}}$  values were obtained by cyclic voltammetry in a potential widow in the non-Faradaic region ( $\text{OCP} \pm 50 \text{ mV}$ ) at different scan rates (10, 20, 30, 40, 50, 60, 70 mV s<sup>-1</sup>). Fitting half  $\Delta j$  ( $\Delta j = j_a - j_c$ ) against the scan rate, the liner slope is the  $C_{\text{dl}}$  value. Where  $j_a$  and  $j_c$  are anodic current density and cathodic current density at OCP, respectively.

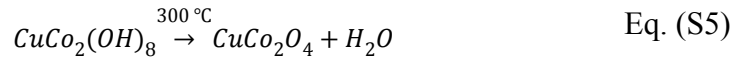
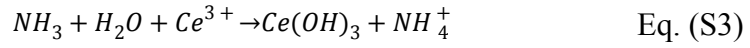
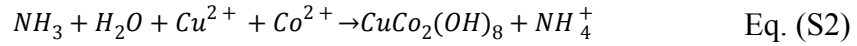
To estimate the Faradaic efficiency of self-supported CeO<sub>2</sub>-CuCoO/NF, a homemade device was made to measure the evolution of H<sub>2</sub> and O<sub>2</sub> gas at a constant current density of 10 mA cm<sup>-2</sup>. The quantity of produced H<sub>2</sub> and O<sub>2</sub> gas was determined by the its volume. The theoretical yields of H<sub>2</sub> and O<sub>2</sub> were calculated by the equations as following <sup>2</sup>:

$$V_{H_2}(\text{mL}) = Q(\text{C}) \times 22.4(\text{L mol}^{-1}) \times 1000/2F(\text{C mol}^{-1})$$

$$V_{O_2}(\text{mL}) = Q(\text{C}) \times 22.4(\text{L mol}^{-1}) \times 1000/4F(\text{C mol}^{-1})$$

Where  $Q = I \times t$ , which means the quantity of electric charge. F is Faraday's constant which equals to 96485.3383 C mol<sup>-1</sup>. The Faradaic efficiency was estimated by comparing the amount of experimentally quantified volume of H<sub>2</sub> and O<sub>2</sub> gas with theoretically calculated gas volume.

### 1.2 Main reactions during the CeO<sub>2</sub>-CuCoO synthesis process:



## S2. More calculation details

### 2.1 Oxygen evolution reaction on the surface

In alkaline conditions, the OER process could occur in the following four steps<sup>3</sup>:



Where \* denotes the active site on the catalyst, OH\*, O\*, and OOH\* stand for the corresponding adsorbed intermediates. The adsorption energy of intermediates (OH\*, O\* and OOH\*) on substrate were calculated following the approach of Nøeskov et al.

4:

$$\Delta E_{OH^*} = E_{OH^*} - E_* - (E_{H_2O} - 1/2E_{H_2}) \quad \text{Eq. (S11)}$$

$$\Delta E_{O^*} = E_{O^*} - E_* - (E_{H_2O} - 1/2E_{H_2}) \quad \text{Eq. (S12)}$$

$$\Delta E_{OOH^*} = E_{OOH^*} - E_* - (2E_{H_2O} - 3/2E_{H_2}) \quad \text{Eq. (S13)}$$

Where  $E_{OH^*}$ ,  $E_{O^*}$ , and  $E_{OOH^*}$  denote the total energy of OH\*, O\*, and OOH\* adsorbed on the surfaces, respectively.  $E_*$ ,  $E_{H_2O}$ , and  $E_{H_2}$  corresponding to the energy of the surface, water, and hydrogen in gas phase. It is well known to us that the energy of intermediates OH\* and OOH\* is very similar because of the same adsorbed sites, and there is an approximately constant difference of  $\Delta E_{OOH^*} - \Delta E_{OH^*}$ , 3.2 eV based on existing studies<sup>5</sup>. Therefore, we directly quote this conclusion in this work. Thus, the free energy of OER is computed by the following equation:

$$\Delta G = \Delta E + \Delta E_{ZPE} - T\Delta S \quad \text{Eq. (S14)}$$

Where  $\Delta E$  is the adsorption energy,  $\Delta E_{ZPE}$  is the zero point energy difference, and  $T\Delta S$  is the corresponding entropy change. Based on recent reported works, the ZPE corrections were obtained from vibrational frequencies, and the vibrational frequencies of O–O and O–H bonds do not change significantly for different metal oxide substrates<sup>6</sup>. The entropic contributions for gaseous molecules are taken from standard

thermodynamics tables. Herein, we use the zero-point energy and entropic contributions to the free Energies as calculated by J.K. Nørskov et al, 0.35, 0.05 and 0.4 eV for adsorbed OH\*, O\*, OOH\* respectively <sup>7,8</sup>. Thus, the free energy change for all OER steps ( $\Delta G_{1-4}$ ) can be expressed as:

$$\Delta G_1 = \Delta G_{OH^*} \quad \text{Eq. (S15)}$$

$$\Delta G_2 = \Delta G_{O^*} - \Delta G_{OH^*} \quad \text{Eq. (S16)}$$

$$\Delta G_3 = \Delta G_{OOH^*} - \Delta G_{O^*} \quad \text{Eq. (S17)}$$

$$\Delta G_3 = 4.92 - \Delta G_{OOH^*} \quad \text{Eq. (S18)}$$

The free energy of H<sub>2</sub>O ( $\Delta G_{H_2O}$ ) and O<sub>2</sub> ( $\Delta G_{O_2}$ ) is taken as zero and 4.92 eV <sup>9</sup>, respectively. The step with the most positive free energy difference is therefore the rate determining step. Therefore, the overpotential  $\eta$  is defined in Eq. (S15):

$$\eta_{theory} = \max\{\Delta G_1, \Delta G_2, \Delta G_3, \Delta G_3\}/e - 1.23 \text{ V} \quad \text{Eq. (S19)}$$

## 2.2 Hydrogen evolution reaction on the surface

The free energy of adsorbed H ( $\Delta G_{H^*}$ ) can represent the HER activity and the  $\Delta G_{H^*}$  can be calculated as:

$$\Delta G_{H^*} = \Delta E_{H^*} + \Delta E_{ZPE} - T\Delta S \quad \text{Eq. (S20)}$$

Where  $\Delta E_{H^*}$  is the absorption energy of H species,  $\Delta E_{ZPE}$  and  $T\Delta S$  are the energy change in zero point energy and entropy, respectively, and T represents the temperature.  $\Delta E_{ZPE}$  and  $\Delta S$  can be calculated as:

$$\Delta E_{ZPE} = E_{ZPE-H^*} - 1/2E_{ZPE-H_2} \quad \text{Eq. (S21)}$$

$$\Delta S = S_{H^*} - 1/2S_{H_2} \quad \text{Eq. (S22)}$$

For H adsorption,  $E_{ZPE-H^*}$  values of metal oxide substrates are calculated to be closed to 0.18 eV with deviations  $<0.01$  eV, and  $E_{ZPE-H_2}$  value is 0.273 eV at standard conditions. When  $S_{H^*}$  is neglected,  $\Delta S \approx -1/2S_{H_2}$ , where  $S_{H_2}$  is the entropy of  $H_2$  in the gas phase at standard conditions. For the  $S_{H_2}$  is 0.4 eV at standard conditions,  $T\Delta S_{H_2}$  is calculated to be -0.2 eV. Therefore, the  $\Delta E_{ZPE} - T\Delta S$  term in equ.1 is set to 0.25 eV.

In addition, the calculations for systems without Ce were also performed by using the Vienna ab initio simulation package (VASP)<sup>10,11</sup>. The obtained data are consistent with the results calculated by DMol3 with thermal converged, indicating that the calculation results obtained by the method used in this work are relatively reliable.

## Additional figures and tables

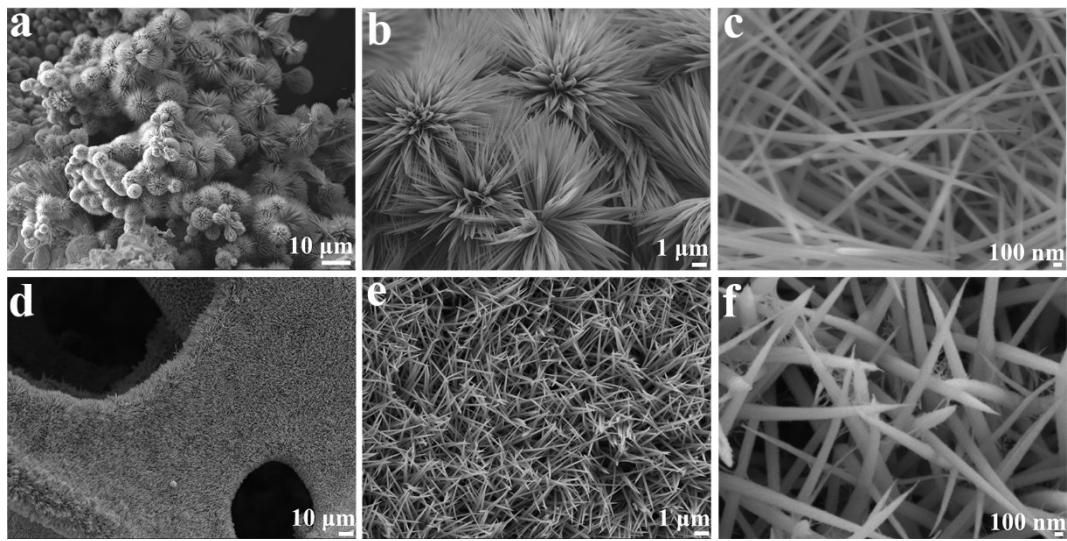


Figure S1. (a, b, c) FESEM images of CeO<sub>2</sub>-CuCoO/NF. (d, e, f) FESEM images of CuCoO/NF.

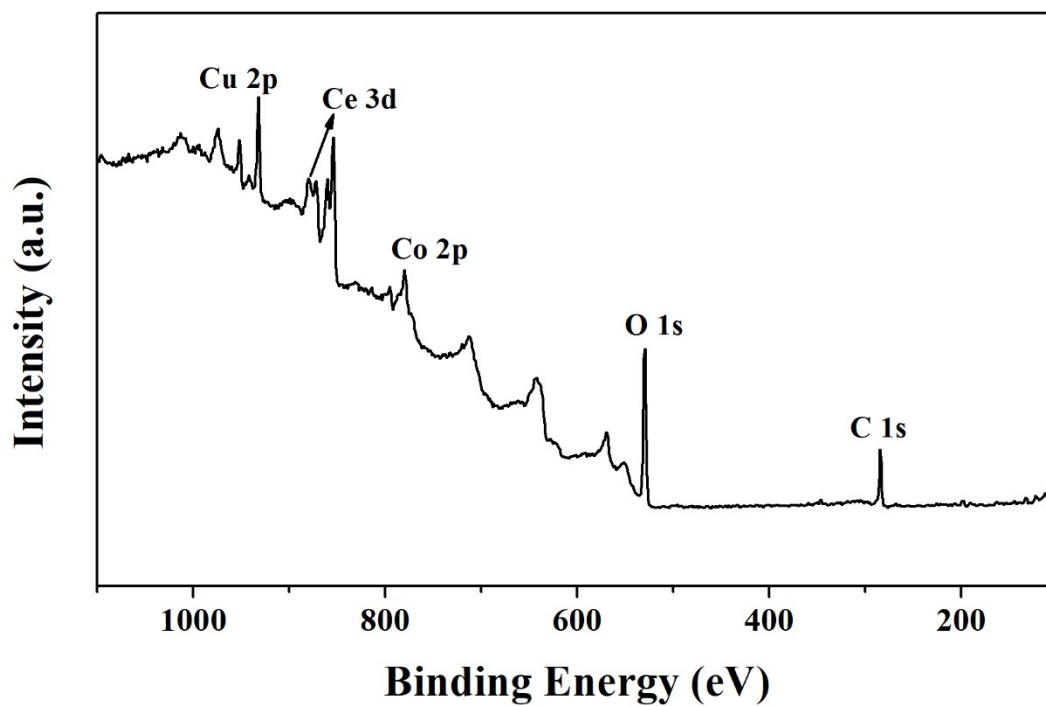


Figure S2. Survey spectrum of CeO<sub>2</sub>-CuCoO/NF.

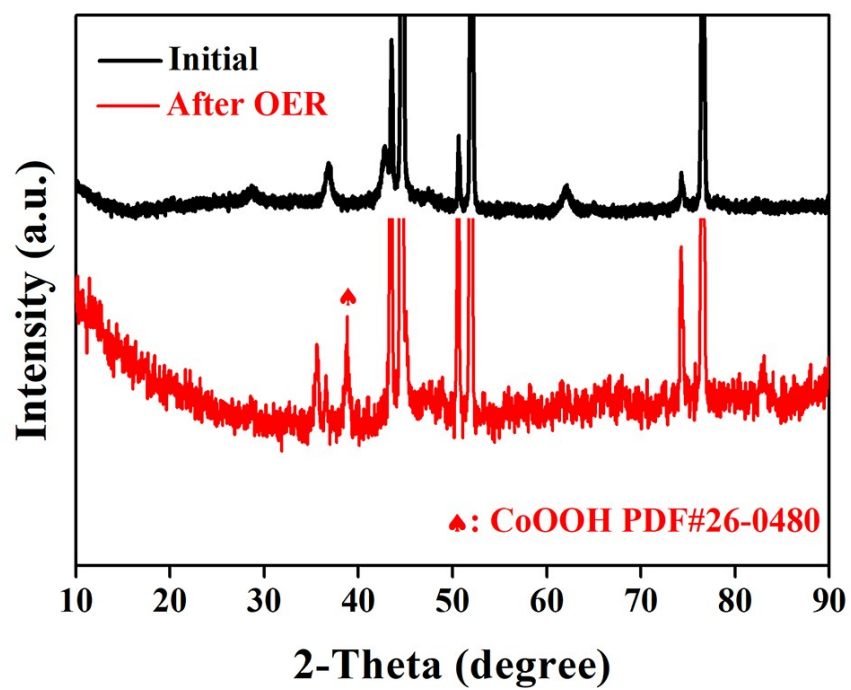


Figure S3 XRD patterns of CeO<sub>2</sub>-CuCoO/NF before and after OER stability test.

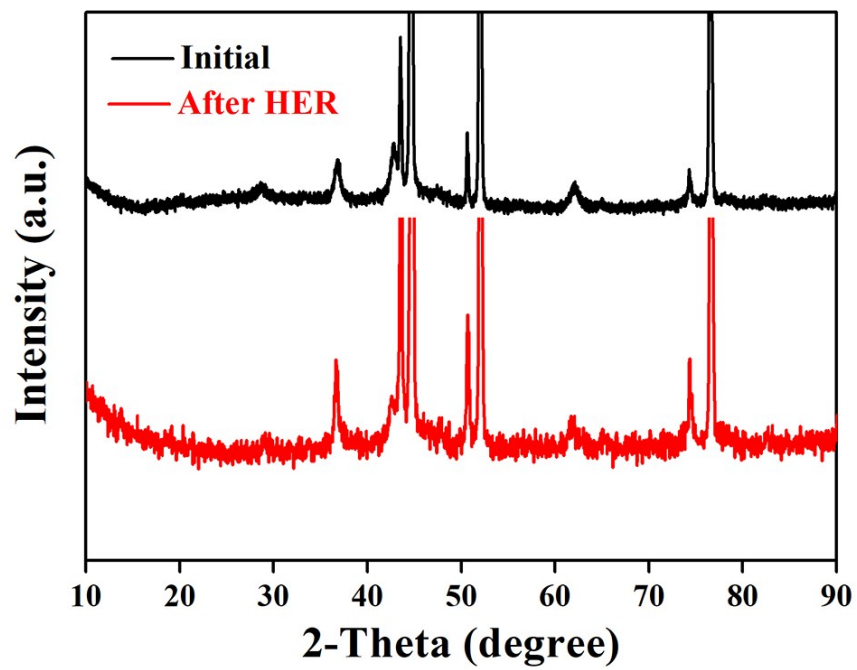


Figure S4 XRD patterns of CeO<sub>2</sub>.CuCoO/NF before and after HER stability test.

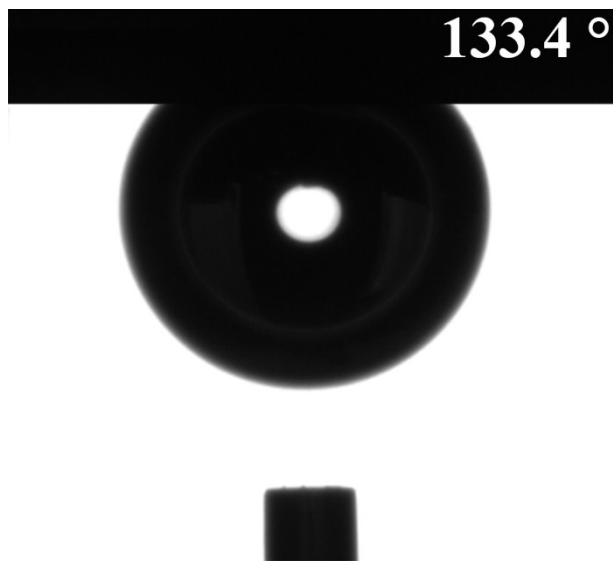


Figure. S5. Bubble contact angle of CuCoO/NF.

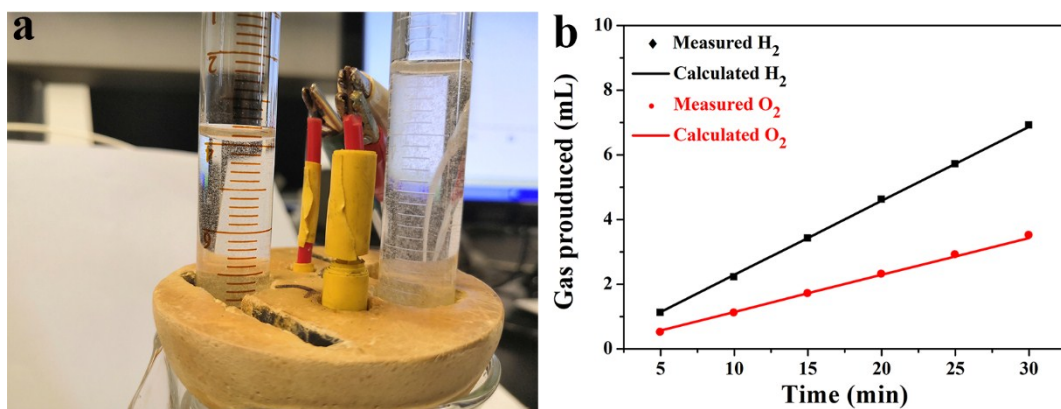
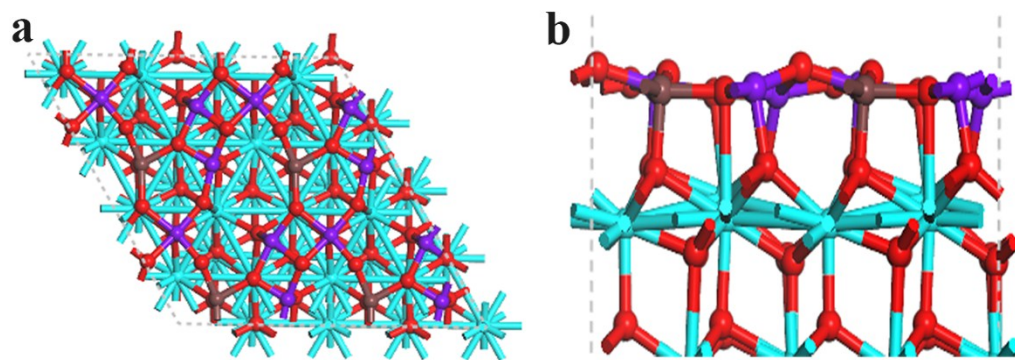


Figure S6. (a) Homemade device directly testing the amount of gas produced during electrolysis.

(b) H<sub>2</sub> and O<sub>2</sub> gas produced.



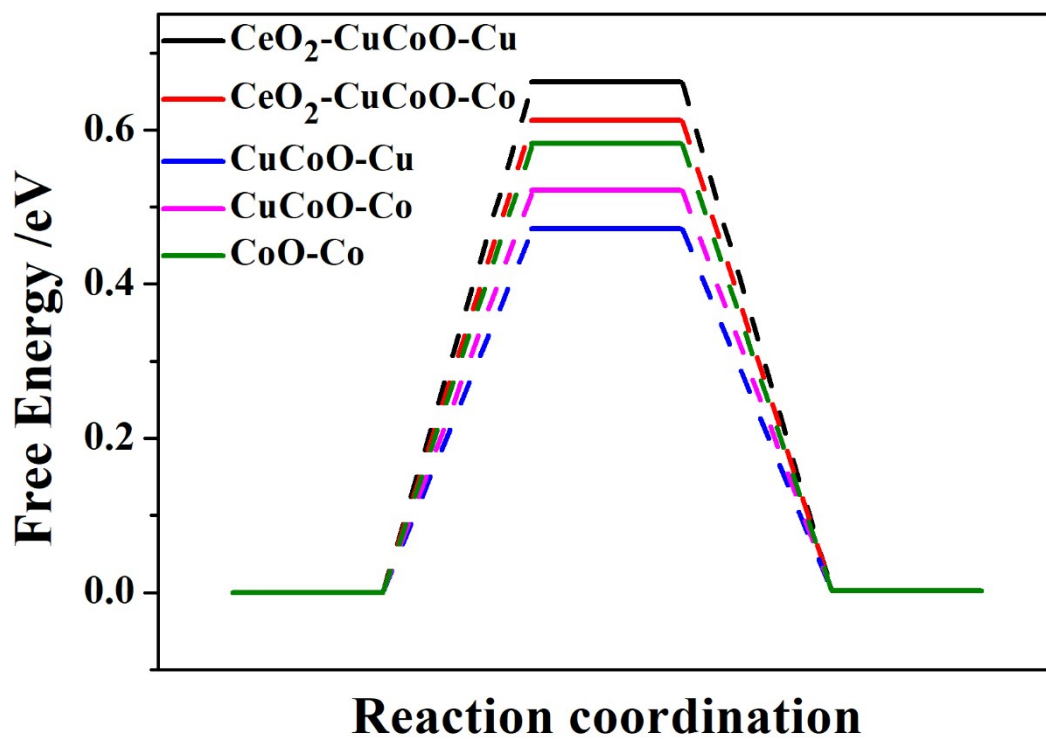


Figure S8. Free energy diagram for hydrogen (H\*) adsorption on CeO<sub>2</sub>-CuCoO, CuCoO, and CoO surface.

Table S1. Comparison of OER activity of CeO<sub>2</sub>-CuCoO/NF with recently reported catalysts in 1.0 M KOH.

Catalysts	Mass loading (mg cm <sup>-2</sup> )	$\eta_{10}$ (mV vs. RHE)	Tafel slope (mV dec <sup>-1</sup> )	References
CeO <sub>2</sub> -CuCoO/NF	1.0	266	58	This Work
SrCo <sub>0.85</sub> Fe <sub>0.1</sub> P <sub>0.05</sub> O <sub>3-<math>\delta</math></sub> /NF	0.034	310	55	12
BSCF/NF	0.039	340	n.a.	13
Co <sub>3</sub> O <sub>4</sub> /NF	1.5	390	82	14
NdBaMn <sub>2</sub> O <sub>5.5</sub> /GC	0.4	400	75	15
Ni <sub>0.9</sub> Fe <sub>0.1</sub> O <sub>X</sub> /QCM	0.01	336	30	16
SNCF-NR	0.464	370	48	17
VOOH nanosphere/NF	0.8	270	68	18
Co <sub>3</sub> O <sub>4</sub> nanorods	2.2	275	n.a.	19
Co-P-S/NF	5.3	283	61	20

Table S2. Comparison of HER activity of CeO<sub>2</sub>-CuCoO/NF with recently reported catalysts in 1 M KOH.

Catalysts	Mass loading (mg cm <sup>-2</sup> )	$\eta_{10}$ (mV vs. RHE)	Tafel slope (mV dec <sup>-1</sup> )	References
CeO <sub>2</sub> -CuCoO/NF	1.0	93	154	This Work
SrCo <sub>0.85</sub> Fe <sub>0.1</sub> P <sub>0.05</sub> O <sub>3-<math>\delta</math></sub> /NF	0.034	110	94	12
NdBaMn <sub>2</sub> O <sub>5.5</sub> /GC	0.4	290	87	15
CoSn <sub>2</sub> /NF	n.a.	103	n.a.	21
NiCoP films/SCW	4.01	178	n.a.	22
Ni <sub>1.5</sub> Fe <sub>0.5</sub> P/CF	1.38	158	n.a.	23
NiCo <sub>2</sub> O <sub>4</sub> /NF	1.0	110	50	24
Cu <sub>0.3</sub> Co <sub>2.7</sub> P/NC	0.4	220	n.a.	25
Co-Ni-B@NF	n.a.	205	n.a.	26
L <sub>0.5</sub> BSCF/rGO	0.5	144	46	27

Table S3. Comparison of electrocatalytic performances of CeO<sub>2</sub>-CuCoO/NF with other reported electrocatalysts for overall water splitting in a 2-electrode electrolyzer.

Catalyst	Mass loading (mg cm <sup>-2</sup> )	Current density (mA cm <sup>-2</sup> )	Potential(V)	Reference
CeO <sub>2</sub> -CuCoO/NF	1.0	10	1.63	This Work
SrCo <sub>0.85</sub> Fe <sub>0.1</sub> P <sub>0.05</sub> O <sub>3-δ</sub> /NF	0.034	10	1.66	12
Co <sub>3</sub> O <sub>4</sub> nanorods	2.2	10	1.72	19
NiCo <sub>2</sub> O <sub>4</sub> /NF	1.0	10	1.65	24
Co-Ni-B/NF	n.a.	10	1.72	26
NiFe LDHs	n.a.	10	1.70	28
NiCo <sub>2</sub> S <sub>4</sub> NW/NF	n.a.	10	1.63	29
Co <sub>0.85</sub> Se/NiFeLDH	4.0	10	1.67	30
NiFe/NiCo <sub>2</sub> O <sub>4</sub> /NF	n.a.	10	1.67	31
NiFe@NC/NF	0.2	10	1.81	32

## References

1. X. Su, Q. Sun, J. Bai, Z. Wang, C. Zhao, *Electrochim. Acta* 2018, 260, 477-482.
2. H. Q. Zhou, F. Yu, Q. Zhu, J. Y. Sun, F. Qin, L. Yu, J. M. Bao, Y. Yu, S. Chen, Z. F. Ren, *Energy Environ. Sci.* 2018, 11, 2858-2864.
3. W. G. Hardin, D. A. Slanac, X. Wang, S. Dai, K. P. Johnston, K. J. Stevenson, J. Highly Active, *Phys. Chem. Lett.* 2013, 4, 1254-1259.
4. X. L. Wang, L. Z. Dong, M. Qiao, Y. J. Tang, J. Liu, Y. Li, S. L. Li, J. X. Su, Y. Q. Lan, *Angew. Chem. Int. Ed.* 2018, 57, 9660-9664.
5. Y. Wang, W. Qiu, E. Song, F. Gu, Z. Zheng, X. Zhao, Y. Zhao, J. Liu, W. Zhang, *Natl. Sci. Rev.* 2018, 5, 327-341.
6. P. Liao, J. A. Keith, E. A. Carter, *J. Am. Chem. Soc.* 2012, 134, 13296-13309.
7. E. Fabbri, A. Habereder, K. Waltar, R. Kötz, T. J. Schmidt, *Catal. Sci. Technol.* 2014, 4, 3800-3821.
8. K. Liu, F. Wang, P. He, T. A. Shifa, Z. Wang, Z. Cheng, X. Zhan, J. He, *Adv. Energy Mater.* 2018, 8, 1703290.
9. J. K. Nørskov, J. Rossmeisl, A. Logadottir, L. Lindqvist, J. R. Kitchin, T. Bligaard, H. Jonsson, *J. Phys. Chem. B* 2004, 108, 17886-17892.
10. G. Kresse, J. Furthmüller, *Computational Materials Science* 2004, 6, 15-50.
11. G. Kresse, J. Furthmüller, *Phys. Rev. B* 1996, 54, 11169-11186.

12. G. Chen, Z. Hu, Y. Zhu, B. Gu, Y. Zhong, H. J. Lin, C. T. Chen, W. Zhou, Z. Shao, *Adv. Mater.* 2018, 30, 1804333.
13. G. Chen, W. Zhou, D.-Q. Guan, J. Sunarso, Y.-P. Zhu, X.-F. Hu, W. Zhang, Z.-P. Shao, *Sci. Adv.* 2017, 3, e1603206.
14. Y. Zhang, B. Ouyang, J. Xu, G. Jia, S. Chen, R. S. Rawat, H. J. Fan, *Angew. Chem. Int. Ed.* 2016, 55, 8670-8674.
15. J. Wang, Y. Gao, D. Chen, J. Liu, Z. Zhang, Z. Shao, F. Ciucci, *ACS Catal.* 2018, 8, 364-371.
16. L. Trotochaud, J. K. Ranney, K. N. Williams, S. W. Boettcher, *J. Am. Chem. Soc.* 2012, 134, 17253-17261.
17. Y. Zhu, W. Zhou, Y. Zhong, Y. Bu, X. Chen, Q. Zhong, M. Liu, Z. Shao, *Adv. Energy Mater.* 2017, 7, 1602122.
18. H. Shi, H. Liang, F. Ming, Z. Wang, *Angew. Chem. Int. Ed.* 2017, 56, 588-592.
19. G. Cheng, T. Kou, J. Zhang, C. Si, H. Gao, Z. Zhang, *Nano Energy* 2017, 38, 155-166.
20. F. Du, Y. Zhang, H. He, T. Li, G. Wen, Y. Zhou, Z. Zou, *J. Power Sources* 2019, 431, 182-188.
21. P. W. Menezes, C. Panda, S. Garai, C. Walter, A. Quiet, M. Driess, *Angew. Chem. Int. Ed.* 2018, 57, 15237-15242.
22. V. R. Jothi, R. Bose, H. Rajan, C. Jung, S. C. Yi, *Adv. Energy Mater.* 2018, 8, 1802615.
23. H. Huang, C. Yu, C. Zhao, X. Han, J. Yang, Z. Liu, S. Li, M. Zhang, J. Qiu, *Nano Energy* 2017, 34, 472-480.

24. X.-H. Gao, H.-X. Zhang, Q.-G. Li, X.-G. Yu, Z.-L. Hong, X. -W. Zhang, C. -D Liang, Z. Lin, *Angew. Chem. Int. Ed.* 2016, 55, 6290-6294.
25. J. Song, C. Zhu, B. Z. Xu, S. Fu, M. H. Engelhard, R. Ye, D. Du, S. P. Beckman, Y. Lin, *Adv. Energy Mater.* 2017, 7, 1601555.
26. N. Xu, G. Cao, Z. Chen, Q. Kang, H. Dai, P. Wang, *J. Mater. Chem. A* 2017, 5, 12379-12384.
27. B. Hua, M. Li, Y.-Q. Zhang, Y.-F. Sun, J.-L. Luo, *Adv. Energy Mater.* 2017, 7, 1700666.
28. J.-S. Luo, J. Im, M. T. Mayer, Marcel Schreier, M. K. Nazeeruddin, N. Park, S. D. Tilley, H.-J. Fan, M. Grätzel, *Science* 2014, 345, 1593-1595.
29. A. Sivanantham, P. Ganesan, S. Shanmugam, *Adv. Funct. Mater.* 2016, 26, 4661-4672.
30. Y. Hou, M. R. Lohe, J. Zhang, S. Liu, X. Zhuang, X. Feng, *Energy Environ. Sci.* 2016, 9, 478-483.
31. C. Xiao, Y. Li, X. Lu, C. Zhao, *Adv. Funct. Mater.* 2016, 26, 3515-3523.
32. Z. Zhang, Y. Qin, M. Dou, J. Ji, F. Wang, *Nano Energy* 2016, 30, 426-433.